Treatment of Human Cells with N-Nitroso(acetoxymethyl)methylamine: Distribution Patterns of Piperidine-Sensitive DNA Damage at the Nucleotide Level of Resolution Are Related to th...

ARTICLE *in* CHEMICAL RESEARCH IN TOXICOLOGY · OCTOBER 1999

Impact Factor: 3.53 · DOI: 10.1021/tx990025f · Source: PubMed

3 AUTHORS:

Jean-François Cloutier
Laval University
9 PUBLICATIONS **187** CITATIONS
SEE PROFILE

Régen Drouin
Université de Sherbrooke
167 PUBLICATIONS **3,218** CITATIONS
SEE PROFILE

Andre Castonguay
Laval University
131 PUBLICATIONS **3,586** CITATIONS
SEE PROFILE

Treatment of Human Cells with *N*-Nitroso(acetoxymethyl)methylamine: Distribution Patterns of Piperidine-Sensitive DNA Damage at the Nucleotide Level of Resolution Are Related to the Sequence Context

Jean-François Cloutier,[†,‡] Régen Drouin,[‡] and Andre Castonguay*[,†]

Laboratory of Cancer Etiology and Chemoprevention, Faculty of Pharmacy, Laval University, Quebec City, Québec G1K 7P4, Canada, and Division of Pathology, Department of Medical Biology, Faculty of Medicine, Laval University, and Unité de recherche en génétique humaine et moléculaire, Research Centre, Pavillon St-François d'Assise, Centre Hospitalier Universitaire de Québec, Québec, Québec, Canada

Received February 8, 1999

The nitrosamine 4-(methylnitrosamino)-1-(3-pyridyl)-1-butanone (NNK) present in tobacco smoke is a major carcinogen involved in tobacco-induced lung cancer. Its complex bioactivation along two pathways, which leads to methylation and pyridyloxobutylation of DNA, makes the study of NNK-induced DNA damage difficult. We selected two nitroso compounds, *N*-methyl-*N*-nitrosourea (MNU) and *N*-nitroso(acetoxymethyl)methylamine (NDMAOAc), with which to map NNK-induced DNA methylation frequency at every nucleotide position. We address the issue of how sequence context and complex chromatin structures, present in living cells, regulate the formation of modified purines through methylation generated by MNU and NDMAOAc. For comparison purposes, purified DNA was treated with dimethyl sulfate (DMS). We used ligation-mediated polymerase chain reaction to map and conduct a high-resolution footprinting analysis of the DNA damage along the *p53* gene (exons 5−8), the *ras* gene family (exons 1 and 2 of H-, K-, and N-*ras* genes), and the c-*jun* promoter in living cells. The distribution of piperidine-sensitive DNA damage induced in cellular DNA and purified DNA by MNU or NDMAOAc was identical. MNU and NDMAOAc methylate more frequently the central guanines in a run of guanines, suggesting a regioselective mechanism for DNA methylation. In contrast, DMS methylates more frequently guanines at the 5′-end of a guanine run; this frequency decreased from the 5′- to the 3′-end. While the presence of adenines in a guanine run does not affect the distribution pattern, the presence of pyrimidines does change said pattern. Our data lead us to suggest that NNK would also methylate DNA sequences in a way similar to that of MNU or NDMAOAc. Footprinted areas of DNA methylated with MNU or NDMAOAc correspond to a consensus sequence for transcription factors AP-1, NF-Jun, CCAAT box, SP-1, and RSRF, as observed in c-*jun* promoters. Our results are in line with the fact that NNK metabolites, generated through the α-hydroxylation pathways, could potentially be mutagenic, since these activated metabolites can methylate guanines. In *p53* and *ras* genes, the frequency of methylation of guanines parallels the frequency of mutations of those same guanines in lung cancer.

Introduction

A series of events initiated by smoke carcinogens produce lesions in lung cells. These lesions can induce mutations, which lead to lung cancer. The mutation spectrum found in lung tumors is determined by four sequential steps of mutagenesis predicted by the theory of somatic mutation (*1*). These four steps are initial lesion frequency (DNA damage), repair rate, polymerase misreading, or misincorporation rate and selection. Our understanding of the whole mutagenic process depends on the full comprehension of each step. The first two steps, taken together, determine to a large extent the frequency of unrepaired lesions encountered by DNA polymerase. Some nucleotides of a gene can be damaged more frequently than others and are called hotspots for damage. The lesion frequency at a specific nucleotide is an important determinant in its contribution to the whole process of tumorigenesis. At a given nucleotide position, the frequency of unrepaired lesions must be relatively high to be frequently mutated (*2*). When the fact that different mutagens induce different mutational spectra is considered, the mutational spectra in a particular type of tumors should reflect the mutagen involved in its induction (*3*).

* To whom all correspondence should be addressed: Laboratory of Cancer Etiology and Chemoprevention, Faculty of Pharmacy, Laval University, Quebec City, Québec G1K 7P4, Canada. Telephone: (418) 656-2131 ext. 3182. Fax: (418) 656-2305. E-mail: andre.castonguay@pha.ulaval.ca.

† Faculty of Pharmacy, Laval University.

‡ Faculty of Medicine, Laval University, and Centre Hospitalier Universitaire de Québec.

10.1021/tx990025f CCC: $18.00
Published on Web 08/31/1999

Scheme 1. Pathways of DNA Methylation by DMS, MNU, or NDMAOAc

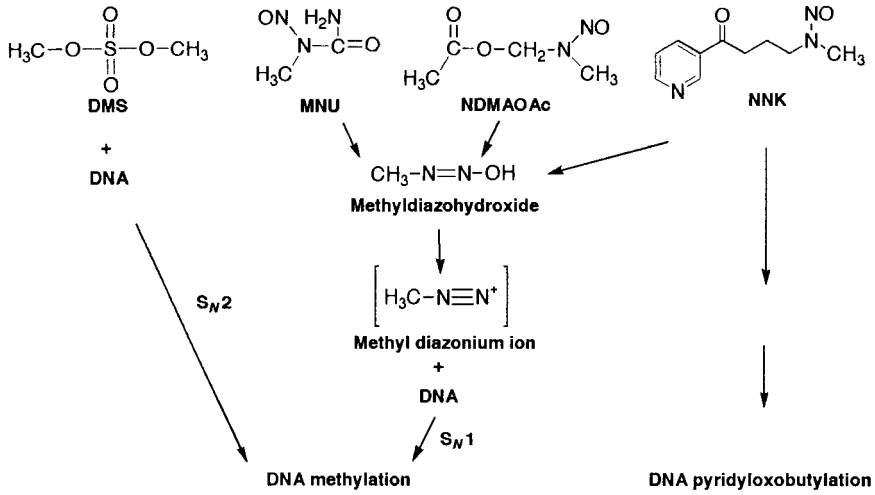

Smoke from American, Canadian, and European cigarettes contains 4-(methylnitrosamino)-1-(3-pyridyl)-1-butanone (NNK),[1] which could be an important etiological factor for lung cancer development in tobacco smokers (*4*−*6*). To damage DNA, NNK must undergo metabolic activation by α-hydroxylation, which forms highly reactive electrophilic intermediates (*7*). This hydroxylation generates two reactive intermediates, 4-(3-pyridyl)-4-oxobutane diazohydroxide which pyridyloxobutylates DNA and methyldiazohydroxide which methylates DNA (Scheme 1). It is difficult to study adduct formation from NNK, due to its complex enzymatic activation and its asymmetrical molecular structure. To bypass this problem, we used a precursor agent *N*-nitroso(acetoxymethyl)-methylamine (NDMAOAc). This nitroso compound is known to be hydrolyzed exclusively, with high yield, to methyldiazohydroxide, which methylates at *N*7 and O^6-guanine sites (*8*, *9*). This pattern of methylation should be identical to the pattern observed with NNK.

Several research groups have investigated the sequence specificity of DNA adduct formation on purified DNA fragments or short oligonucleotides by various methylating agents (*9*−*15*). The base specificity and sequence specificity of adduct formation, analyzed previously with end-labeled DNA fragments inserted in plasmid DNA, could be different than those in genomic DNA sequences in living cells. It has been shown that the susceptibility of forming *N*7-methylguanine and O^6-methylguanine in purified DNA or in cellular DNA treated with *N*-methyl-*N*-nitrosourea (MNU) is modulated by the DNA structure (*10*, *16*, *17*). Particular damage to DNA is not uniform along gene sequences, and the DNA damage distribution in living cells is determined by the sequence context and the chromatin effects (*18*). It is therefore not known how complex DNA structures or protein−DNA interactions in living cells display sequence specificity in methylation patterns with NDMAOAc. We present a more realistic description of DNA damage distribution occurring in living cells. In this paper, global frequency means the genomic average formation frequency of a DNA adduct, e.g., one methylated guanine per 5 kb of DNA sequence. DNA adduct distribution represents the frequency of methylated guanine formation at each nucleotide position of a defined DNA sequence; DNA adduct distribution pattern refers to the methylated guanine frequency of all nucleotide positions of DNA fragments.

In this study, we used ligation-mediated polymerase chain reaction (LMPCR) to map along the DNA sequence in purified DNA and in cellular DNA (cell culture treatment) piperidine-sensitive MNU and NDMAOAc-induced DNA damage in the *p53* gene, H-*ras*, K-*ras*, and N-*ras* genes, and the c-*jun* promoter. LMPCR is an ultrasensitive method for the mapping of rare DNA strand breaks in a complex genome at the nucleotide level. We determined whether methylation of DNA by MNU and NDMAOAc is affected by the sequence context. Furthermore, we conducted in living cells a high-resolution footprinting analysis of the five genes listed above.

Experimental Procedures

Cell Culture and Methylating Agent Treatments. Human skin fibroblasts were grown to confluence in Dulbecco's modified Eagle's medium (DMEM) (Gibco BRL, Burlington, ON) supplemented with 5% fetal bovine serum (FBS) (Gibco BRL). The culture medium was replaced with fresh unsupplemented DMEM containing the following methylating agents (living cell treatment): 15 mM MNU (Sigma Chemical Co., St. Louis, MO) or 0.3 mM NDMAOAc (LKT Laboratory, St. Paul, MN). Cells were treated with nitroso compounds (MNU or NDMAOAc) at 37 °C for 2 h. After treatments, the cells were washed with Ca- and Mg-free Hank's balanced salt solution and detached by trypsinization. Nuclei were isolated and their DNAs purified as described by Drouin et al. (*19*) and Pfeifer et al. (*20*), respectively. The concentration of DNA was measured by spectrophotometry at 260 nm. Purified DNA that was extracted from lymphocytes was treated with 21 mM DMS as described by Pfeifer et al. (*21*). For MNU-treated DNA, 30 μg of purified DNA, diluted in 15 mM sodium citrate buffer (pH 7.0) and 2 mM EDTA, was exposed to 8 mM MNU at room temperature, in a final volume of 450 μL, for 30 min. For NDMAOAc treatment of purified DNA, 0.3 mM NDMAOAc and 2 units of esterase (crude extract from porcine liver) (Sigma Chemical Co.) were added to 30 μg of purified DNA diluted in 15 mM sodium citrate buffer (pH 7.0) and 2 mM EDTA in a final volume of 450 μL; treatment was performed as previously described (*22*). After carcinogen treatments, DNA was precipitated as described previously (*19*, *20*).

[1] Abbreviations: DMEM, Dulbecco's modified Eagle's medium; DMS, dimethyl sulfate; FBS, fetal bovine serum; LMPCR, ligation-mediated polymerase chain reaction; MEP, molecular electrostatic potential; MMS, methylmethane sulfonate; MNU, *N*-methyl-*N*-nitrosourea; NDMAOAc, *N*-nitroso(acetoxymethyl)methylamine; NNK, 4-(methylnitrosamino)-1-(3-pyridyl)-1-butanone; RSRF, related to serum response factor.

DNA Damage Conversion to DNA Strand Breaks. After exposure to the methylating agents, DNA was treated with 1 M piperidine at 80 °C for 30 min to convert the methylated bases to DNA strand breaks. The global frequency in total genomic DNA of piperidine-sensitive DNA damage was estimated with an alkaline 1.5% agarose gel (*23*). The methylating agent treatments for cells and naked DNA were established so at least one methylated base per 1 kb was produced. Maxam−Gilbert DNA cleavage reactions were carried out as described previously (*21*, *24*). To specifically modify adenines, DNA was treated with potassium tetrachloropalladate (K_2PdCl_4) at pH 2.0, followed by piperidine treatment (*25*).

LMPCR. Details of the LMPCR protocol used in this study have been published (*19*). The protocol is divided into six steps: (1) primer extension of an annealed gene-specific oligonucleotide (primer 1) to generate blunt ends from nicked genomic DNA, (2) ligation of an universal asymmetric double-strand linker, (3) PCR amplification using a second gene-specific oligonucleotide (primer 2), (4) separation of the DNA fragments on a sequencing polyacrylamide gel, (5) transfer of the DNA to a nylon membrane by electroblotting, and (6) hybridization of a radiolabeled probe prepared by repeated primer extension using a third gene-specific oligonucleotide (primer 3) and a gene-specific DNA template. Starting with 0.8 μg of DNA, primer extension, ligation of the linker, PCR, gel electrophoresis, electroblotting transfer, probe preparation, and hybridization were carried out as usual (*19*, *26*). For each LMPCR protocol, each step was conducted in triplicate for methylating agent and piperidine-treated DNA, and in duplicate for the various controls. After the PCR procedures, half of each sample was loaded on a sequencing polyacrylamide gel for screening. When no significant variation between samples of the same triplicate was observed, the remaining half-samples were pooled. Then, another sequencing gel was repeated with the pooled samples. The nylon membranes (Qiagene, Santa Clarita, CA) were then exposed to a phosphor-sensitive imaging plate (type III-s). Band intensities on the autoradiogram were quantified with a Fuji BAS 1000 phosphorimager (Fuji Medical Systems USA Inc., Stanford, CT) and analyzed with MacBAS 2.5.

Gene Selection. Primers specific for (1) human *p53* gene exons 5−8 and intron 5−exon 5, (2) the c-*jun* promoter, and (3) the human K-*ras*, N-*ras*, and H-*ras* genes and exons 1 and 2 were selected for this study (*27*−*29*). The selected primers covered the nontranscribed strand and the transcribed strand of the genes mentioned above. In total, we have mapped the equivalent of approximately 6.8 kb of the linear single-strand sequence.

Caution: *DMS, MNU, and NDMAOAc should be handled as toxic and potential human carcinogens.*

Results

Piperidine Conversion of Methylated Bases to DNA Strand Breaks. The term alkali-labile lesion is often applied to DNA sites where a guanine residue has been alkylated at its *N*7 position. Maxam and Gilbert proposed a mechanism for piperidine-mediated cleavage of DNA at *N*7-methylguanine sites that involves a displacement of the formamidopyrimidine form of guanine from its deoxyribose moiety by the secondary amine piperidine (*24*). Hot aqueous piperidine provides a basic medium promoting strand cleavage at such sites. The C8−C9 bond of the alkylguanine ruptures under alkaline conditions, and the formamidopyrimidine leads to the labilization of the *N*-glycosylic bond of the resulting opened imidazole ring structure with subsequent formation of an abasic site. Subsequent β-elimination creates breaks in the phosphodiester backbone. Alkaline conditions alone can cause the formation of the formamidopyrimidine structure, but it is less efficient than piperidine at inducing the breakage of the phosphodiester backbone

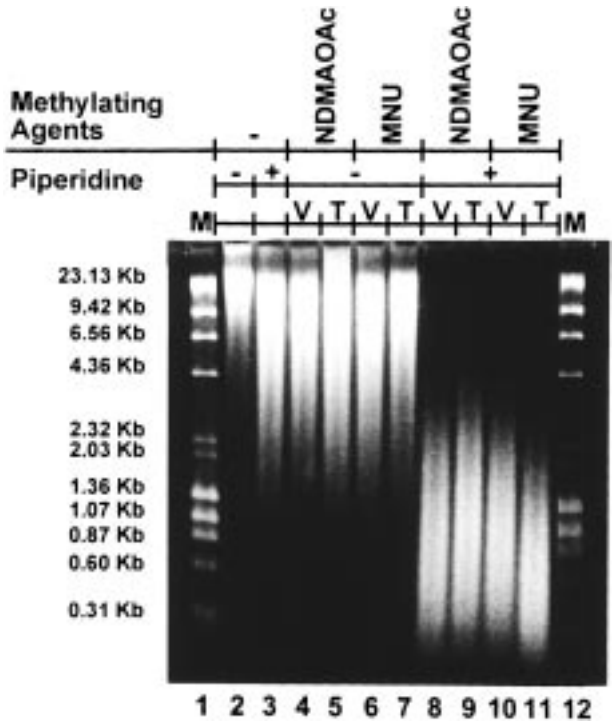

Figure 1. Alkaline agarose gel (1.5%) display of NDMAOAc- and MNU-induced DNA lesion frequency following hot piperidine conversion of DNA damage. The first and last lanes (M) of this gel contained *Hin*dIII λ bacteriophage and ϕX174 DNA molecular weight standards. Lane 2 contained untreated DNA, no methylating agent, and no piperidine. Lane 3 represents piperidine control, no methylating agent with piperidine treatment. Lanes 4−11 contained NDMAOAc- and MNU-treated DNA without (lanes 4−7) or with (8−11) hot piperidine treatment. V means in cell culture, and T means with purified DNA.

at the abasic site (*24*, *30*). It is pertinent to note that *N*3-methyladenines are more stable in aqueous piperidine solutions than *N*7-methylguanines (*30*).

Estimate of Global DNA Damage Frequency Induced by MNU and NDMAOAc. The global adduct frequency is estimated after electrophoresis of single-stranded DNA fragments on a denaturing agarose gel. The migration of DNA fragments through agarose gel separates them according to their size. In such a gel, mobility analysis coincides with the mobility of the maximum peak of ethidium bromide fluorescence. The adduct frequency is correlated with the average size of DNA fragments. In this study, methylating agents have induced single-strand breaks which were estimated in the absence of piperidine treatment. Additional single-strand breaks are generated when methylated DNA is treated with piperidine, converting DNA damage to single-strand breaks. The global adduct frequency, in MNU- or NDMAOAc-treated fibroblasts and naked DNA, following piperidine conversion is estimated to be 22 methylated bases per 10 kb (Figure 1, lanes 8−11). The final concentrations of MNU or NDMAOAc were selected for cell culture or purified DNA conditions, to produce similar adduct frequencies. In the absence of piperidine treatment, MNU or NDMAOAc induces a low level of single-strand breaks, i.e., one DNA strand break per 10 kb (Figure 1, lanes 4−7). Similarly, in the absence of MNU or NDMAOAc, piperidine treatment alone creates one nonspecific DNA strand break per 10 kb (Figure 1, lane 3). Procedures for purification and precipitation of nuclear DNA and the alkaline conditions of the agarose

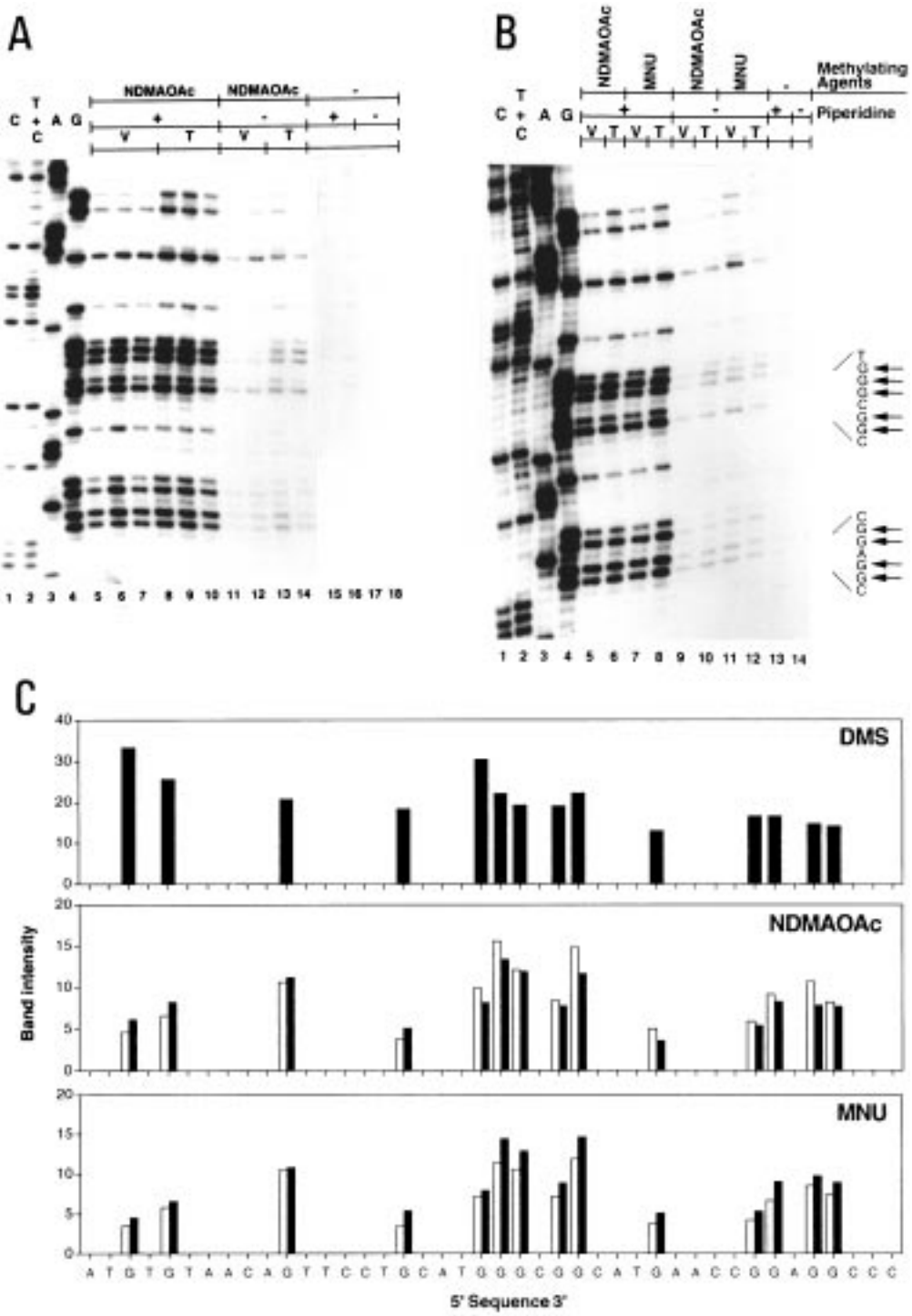

Figure 2. LMPCR analysis of damage induced by NDMAOAc or MNU in the nontranscribed strand (upper strand) of exon 7 of the *p53* gene. The distribution of adducts in *p53* gene was determined after cleavage with hot piperidine and LMPCR. (A) A screening gel of NDMAOAc-treated DNA: lanes 1−4, LMPCR of DNA treated under standard Maxam−Gilbert cleavage reaction conditions; lanes 5−7, 11, and 12, LMPCR of NDMAOAc-treated fibroblasts (V means in cell culture) followed by piperidine treatment (lanes 5−7) or not (lanes 11 and 12); lanes 8−10, 13, and 14, LMPCR with NDMAOAc treatment of purified DNA (T means with purified DNA) followed by piperidine treatment (lanes 8−10) or not (lanes 13 and 14); and lanes 15−18, LMPCR of untreated DNA, followed by piperidine treatment (lanes 15 and 16) or not (lanes 17 and 18). (B) Lanes 1−4, LMPCR of DNA treated under standard Maxam−Gilbert cleavage reaction conditions; lanes 5, 6, 9, and 10, LMPCR of NDMAOAc-treated fibroblasts and purified DNA followed by piperidine treatment (lanes 5 and 6) or not (lanes 9 and 10); lanes 7, 8, 11, and 12, LMPCR of MNU-treated fibroblasts and purified DNA followed by piperidine treatment (lanes 7 and 8) or not (lanes 11 and 12); and lanes 13 and 14, LMPCR of untreated DNA followed by piperidine treatment (lane 13) or not (lane 14). For guidance, a small portion of the Maxam−Gilbert-derived sequence is shown on the right for exon 7, and arrows denote guanines. (C) Densitometry quantification with a phosphorimager of the pooling gel (panel B). Lane 4 shows DMS treatment of purified DNA, and lanes 5−8 show NDMAOAc/MNU treatment of fibroblasts or purified DNA. (■) With purified DNA and (□) in cell culture. Signal intensities were quantified by MacBAS 2.5. Data were normalized with the background measured in each lane.

gel do not produce significant strand breakage, the DNA strand break frequency being less than 0.4 adduct per 10 kb (Figure 1, lane 2). Methylation of purified DNA by DMS, followed by piperidine treatment, produced 40

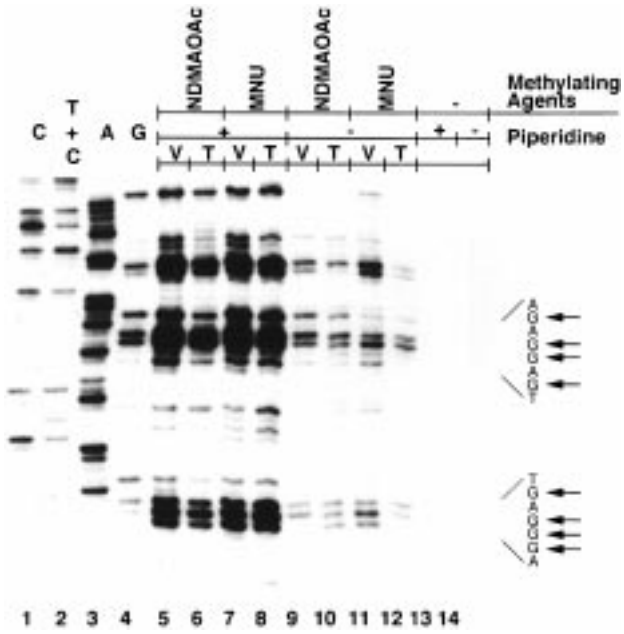

Figure 3. LMPCR analysis of damage induced by NDMAOAc or MNU in the nontranscribed strand (upper strand) in exon 2 of the K-*ras* gene. The distribution of adducts in the K-*ras* gene was determined after cleavage with hot piperidine and LMPCR. Lanes 1−14 are as described in the legend of Figure 2B.

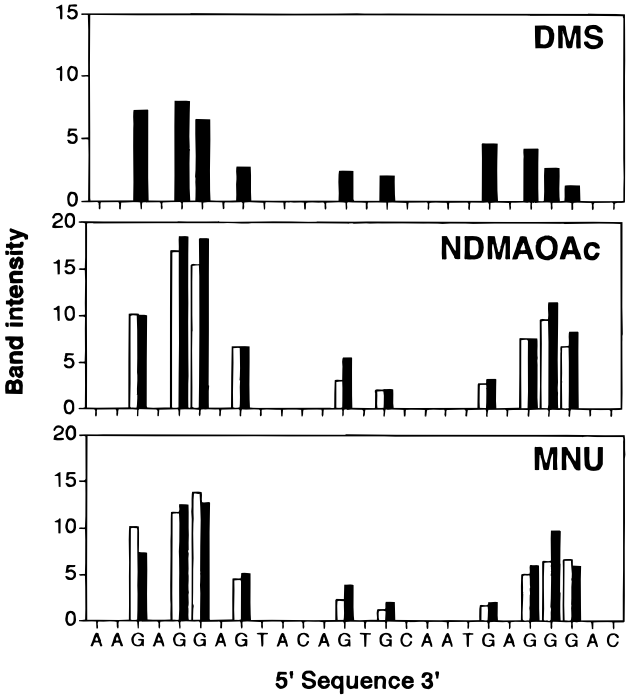

Figure 4. Densitometry quantification with the phosphoimager of DNA damage induced by NDMAOAc or MNU in the nontranscribed strand (upper strand) in exon 2 of the K-*ras* gene (Figure 3). See the legends of Figures 2C and 3 for a detailed description.

lesions per 10 kb (data not shown). The adduct frequency observed in MNU, NDMAOAc, and DMS-treated DNA is suitable for DNA damage distribution analysis by LMPCR.

Distribution of DNA Damage and Sequence Context. The distribution of DNA damage induced by methylating agents in human *p53* gene, in the c-*jun* promoter, and in *ras* genes (K-*ras*, N-*ras*, and H-*ras*) was mapped at the sequence level by LMPCR. In living cells or with purified DNA, methylating agents preferentially methylate guanine residues (Figure 2, panels A and B, and Figures 3, 6, and 8). The hot piperidine cleavage of the DNA phosphate backbone at the site of methylated guanine residues leaves a free 5′-phosphate end. These 5′-phosphate single-strand breaks can be quantitatively mapped at the resolution of a single base by the LMPCR technique coupled with a DNA sequencing gel. No significant variation was observed among samples of the triplicate, indicating that the long LMPCR procedure does not introduce variations due to manipulations and is at least semiquantitative (Figure 2A). Triplicate samples with the same methylating agent dose were selected instead of using three different doses of this agent because the triplicate approach makes it easier to estimate the variation due to manipulations. MNU-treated DNA gave similar results with the screening gel (data not shown). The three agents that were studied methylate bases. However, guanines methylated at the *N*7 position are the methylated bases most easily converted to DNA strand breaks during hot piperidine treatment. The *N*7 position of all guanine residues (Gs) is not methylated with the same efficiency by these three agents. Indeed, many G sites exhibited very intense bands, indicating a very efficient methylation of their *N*7 positions (panels A and B of Figure 2, lanes 3, 6, and 8). Differences in methylation patterns are observed when DMS-treated DNA is compared to MNU- or NDMAOAc-treated DNA (Figures 2C, 4, 7, and 9). The guanine residues in DNA are modified with high sequence selectivity, but there are discernible patterns in the polyG stretches between these compounds. There is a relationship between the methylation efficiency and the identity of the flanking bases. In general, the 3′-base has less of an effect on the methylation pattern than the 5′-base. We observed that DMS preferentially methylates guanines at the 5′-end of a guanine run. The efficiency decreases from 5′-G to 3′-G for DMS (Figure 5). In contrast, MNU and NDMAOAc methylate more frequently central guanines in a run of three or more guanines (Figure 5). The distribution patterns take a bell shape with the outmost 5′- and 3′-Gs being the least efficiently methylated. DNA base damage distribution patterns induced by MNU or NDMAOAc observed in cellular DNA are very similar to those induced in purified DNA (Figure 5). These patterns can be observed with all DNA sequences that were studied. We analyzed guanine runs in which an adenine or pyrimidine (C or T) bases are intercalated (up to three guanines) (Figure 5). When adenines are present in guanine runs (Figure 2C, GGAGG; Figure 4, GAGGAG and GAGGGA; and Figure 9, GGGAAGG), no effect is observed on the damage pattern of the entire purine run. However, when pyrimidines are present, the whole damage pattern is changed in DMS-, MNU-, or NDMAOAc-treated DNA (Figure 2C, GGGCGG; and Figure 7, GGGGGGCGGG). The presence of a pyrimidine breaks the damage distribution pattern of the entire guanine run and leads to the formation of two similar distribution patterns rather than a unique distribution pattern (Figure 5). Furthermore, we noticed a periodicity in the methylation distribution patterns. We observed a variation in the DNA damage distribution patterns on a larger scale in living cells and in purified DNA. As an example in Figure 2C, from 5′ to 3′ we

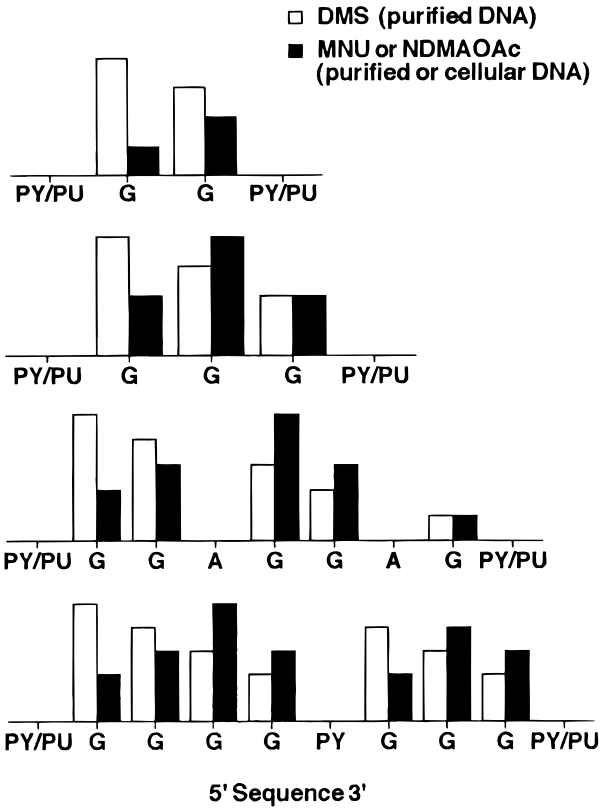

Figure 5. Summary of DNA damage distribution patterns observed in various guanine runs with MNU-, NDMAOAc-, and DMS-treated DNA in cell culture and with purified DNA: (□) DMS (purified DNA) and (■) MNU or NDMAOAc (purified or cellular DNA). PY/PU represents pyrimidine/purine.

observe that the level of damage is low (5′-ATGTGTA), high (ACAGTTC), low (CTGCATG), high (GGCGGCA), low (TGAACCG), and high (GAGGCCC-3′). This periodicity can be observed in each figure. This sinusoidal periodicity is likely to be related to the DNA structures. The low damage frequency is an indication of less accessible guanines, and high damage frequencies are an indication of more accessible guanines.

Footprinting Analysis. When living cells are exposed to methylating agents, guanine residues in contact with sequence-specific DNA-binding proteins exhibit degrees of reactivity with methylating agents that are different from those of guanine residues not in contact with binding proteins. Proteins in contact with DNA either decrease the accessibility of specific guanines to methylating agents, which is defined as protection, or often increase the reactivity at the edge of a protein−DNA contact, which is defined as hyperreactivity (*31*). Hyperreactivity can also reveal a greater accessibility in cellular DNA structures to methylating agents. We have conducted a detailed footprinting analysis of all the selected genes, i.e., the *p53* gene, *ras* genes, and the c-*jun* promoter. Footprinted areas are seen only in the c-*jun* promoter. Footprinted areas correspond to a consensus sequence for transcription factor binding sites. Examples of footprinting in the c-*jun* upstream region to the major transcription factor initiation start are shown in Figures 6 and 8. Several areas of differential hypo- or hyperreactivity between purified and cellular DNA treated with MNU or NDMAOAc are apparent, and indicate protein−DNA contacts or an otherwise altered DNA structure at these sites. These areas correspond to factors AP-1, NF-

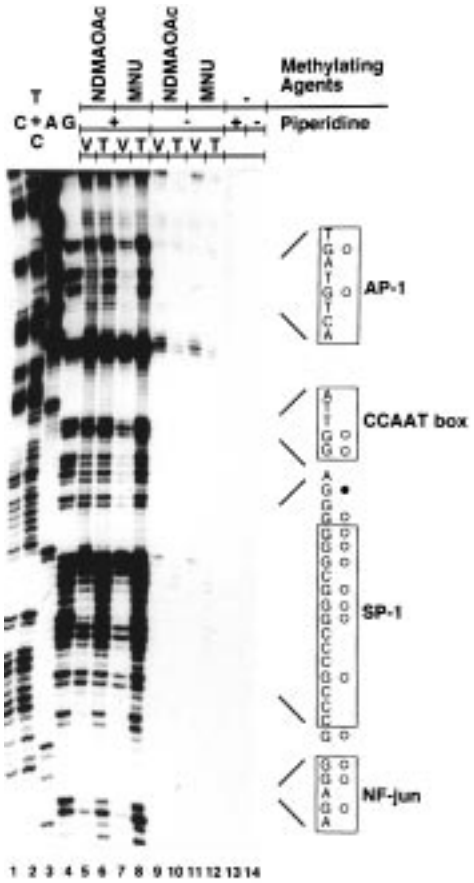

Figure 6. Genomic footprinting of the c-*jun* promoter with NDMAOAc and MNU. The region that is shown was analyzed to reveal lower strand sequences from nucleotides −145 to −56 to the site of major transcription factor initiation. The distribution of adducts in the c-*jun* promoter was determined after cleavage with hot piperidine and LMPCR. White circles indicate those Gs which exhibit cellular protection against NDMAOAc- or MNU-induced modification, and the black circles indicate those exhibiting cellular hyperreactivity. Lanes 1−14 are as described in the legend of Figure 2B.

Jun, CCAAT box, SP-1, and RSRF. The upper section of the autoradiogram in Figure 6 shows a cellular G's hyporeactivity. Hyporeactivity or protection corresponds to the AP-1-like sequence (5′-TGATGTCA-3′) and the CCAAT box binding protein (5′-ATTGG-3′). The lower part of the autoradiogram shows other cellular protection corresponding to the binding site for transcription factor NF-jun (5′-GGAGACTCC-3′), and near this site is the SP-1 consensus sequence (5′-GGGCGGG-3′), where two hyperreactive Gs are flanked by four protected Gs (Figure 6). The CCAAT box binding sequence located at the top of the autoradiogram in Figure 8 corresponds to the complementary sequence (5′-CCAAT-3′) observed in Figure 6. Near this sequence, we observed the complementary sequence of the AP-1-like sequence, i.e., 5′-TGACATCA-3′. The overlap analysis of both strands of the c-*jun* promoter clearly reveals that these factors (CCAAT box and AP-1) are located at the same position in the upstream region and allow more precise definition of the limits of the binding site. Close to the AP-1 sequence, two series of Gs exhibit hyper- and hyporeactivities which correspond to a known consensus sequence for a putative RSRF (related to serum response factor) binding site (Figure 8). The footprints obtained with MNU and NDMAOAc are very similar. In Figure 8, a cellular hyperreactive guanine is observed with MNU- or ND-

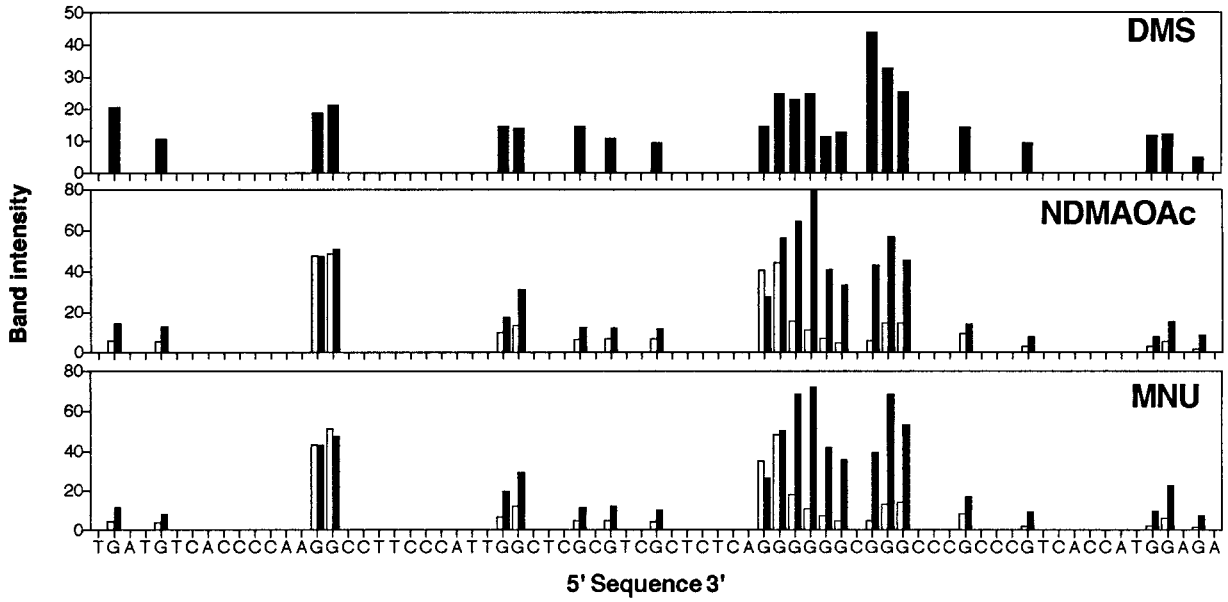

Figure 7. Densitometry quantification with the phosphoimager of DNA damage induced by NDMAOAc or MNU in the c-*jun* promoter (lower strand, Figure 6). See the legends of Figures 2C and 6 for a detailed description.

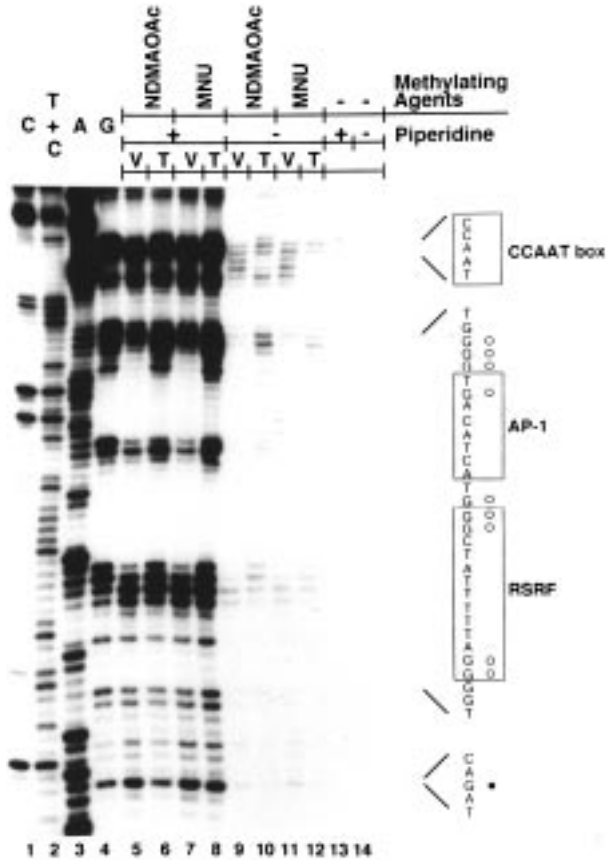

Figure 8. Genomic footprinting of the c-*jun* promoter with NDMAOAc and MNU. The region that is shown was analyzed to reveal the upper strand sequence from nucleotides −86 to −26 to the site of major transcription factor initiation. The distribution of adducts in the c-*jun* promoter was determined after cleavage with hot piperidine and LMPCR. White circles indicate those Gs which exhibit cellular protection against NDMAOAc- or MNU-induced modification, and black circles indicate those exhibiting cellular hyperreactivity. Lanes 1−14 are as described in the legend of Figure 2B.

MAOAc-treated DNA. We observed a higher band intensity with cellular DNA than with purified DNA after NDMAOAc treatment.

Discussion

In contrast to naked DNA, packaged nuclear DNA includes many nuclear proteins. This difference always raises the question of how extensively the sequence selectivities observed in naked DNA can be extrapolated to cells. The yield of methylated guanines in the absence of protein shielding as observed in DMS- or MNU-treated DNA is similar; this suggests that the cellular conditions have no detectable effect on the overall susceptibility of guanines to methylation (*32*). Accordingly, if a DNA sequence is accessible to a methylating agent, the pattern of sequence-dependent reactivity is not grossly affected by the nuclear "milieu". To test whether the sequence specificity is related to chromatin structure, we compared DNA damage patterns in MNU- or NDMAOAc-treated fibroblasts with those observed with purified genomic DNA. When purified DNA and cellular DNA are being compared, the distribution patterns of methylated guanine residues induced by the two methylating agents were almost identical (with the exception of several footprinted areas observed in the c-*jun* promoter); this excludes chromatin structure as a major modulating factor of the DNA methylation pattern (Figures 2 and 3). Our results suggest that the main determinant of MNU- or NDMAOAc-induced DNA damage is the DNA sequence.

Methylating agents are divided into three groups according to their chemical structure: the alkyl sulfate, such as dimethyl sulfate (DMS), the alkyl sulfonate, such as methylmethane sulfonate (MMS), and the *N*-nitroso compounds (MNU, NDMAOAc, and NNK) (*32*). Methylating agents bind to various sites on DNA molecules according to the rules of electrophilicity and nucleophilicity (*32*). DMS and MMS react with DNA by a mechanism of bimolecular nucleophilic substitution (S_N2). S_N2 reactions are strictly dependent upon steric accessibility (Scheme 1). In contrast to DMS and MMS, MNU and NDMAOAc react with DNA by a mechanism of unimolecular nucleophilic substitution (S_N1). This reaction involves the formation of an electrophilic carbocation intermediate which reacts with a nucleophilic center of the DNA, thus forming an adduct (Scheme 1).

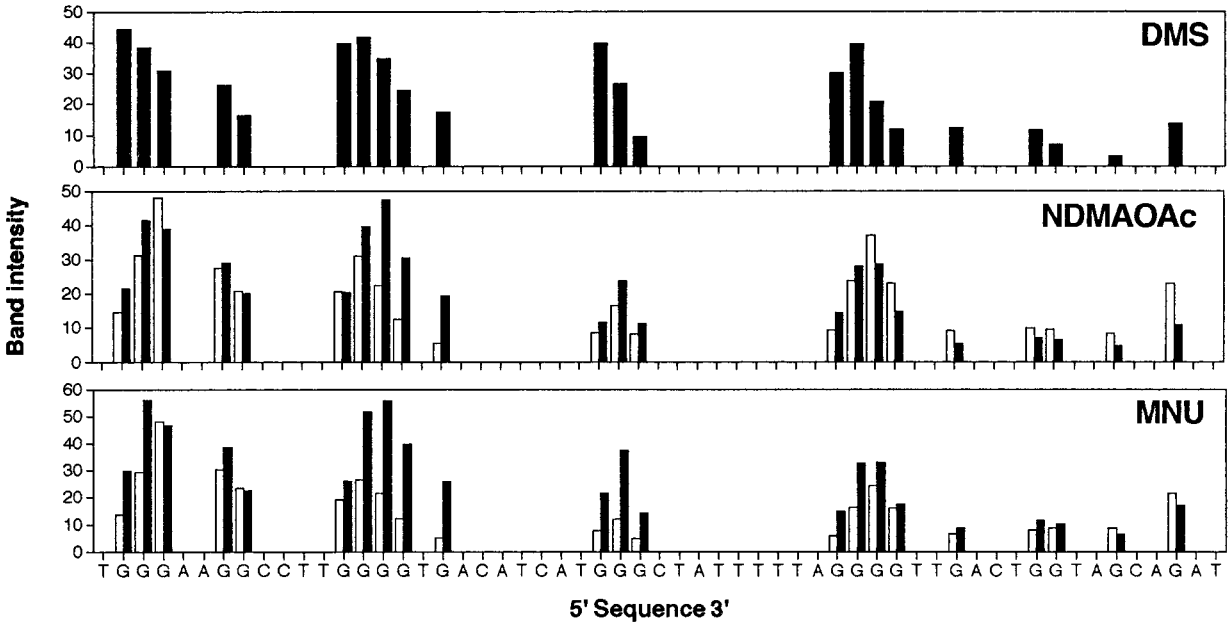

Figure 9. Densitometry quantification with the phosphoimager of DNA damage induced by NDMAOAc or MNU in the c-*jun* promoter (upper strand in Figure 8). See the legends of Figures 2C and 8 for a detailed description.

Several research groups have observed a sequence specificity of DNA adduct formation on purified DNA fragments or short oligonucleotides (*10*−*15*). The ratio of O^6-methylguanine to *N*7-methylguanine was found to be higher in CGC sequence than in GGG sequence in oligonucleotides, indicating that neighboring bases affect the pattern of methylation of guanine by MNU (*10*). In dodecadeoxynucleotides methylated by MNU, levels of O^6- and *N*7-methylguanine were greater when the guanine residue was preceded in 5′ by an adenine, rather than by a thymidine (*11*). In DNA fragments, the intensity of MNU binding to guanine runs revealed that the 3′-neighbors exerted a greater influence than the 5′-neighbors (*14*). We observed that DNA damage induced by MNU or NDMAOAc is sequence-specific in a run of three or more guanines in purified DNA and in cellular DNA (Figure 5). Our results, and those realized by other investigators, confirm that the sequence specificities of S_N1 agents are different from those of S_N2 agents (Figure 5) (*12*−*15*, *33*). S_N1 methylating agents (MNU and NDMAOAc) preferentially methylate the central guanines in a run of three or more guanines. On the other hand, S_N2 agents exhibited preferential methylation at the 5′-end in similar guanine runs. Taken together, these results suggest that the reactivity of individual guanines is determined by the methylating species and by the sequence context. The preference of MNU and NDMAOAc for guanine runs is reminiscent of the alkylation pattern induced by *N*-(2-chloroalkyl)-*N*-nitrosoureas. Hartley et al. (*34*, *35*) showed that *N*-(2-chloroalkyl)-*N*-nitrosoureas preferentially alkylate the middle guanines in runs of three or more guanines.

Factors determining the sequence specificity of guanine methylation could be (1) steric effects, (2) enhancement of the nucleophilicity of the *N*7 position, or (3) a regioselective mechanism involving a previous methylation of the end guanine. The yield of methylation by MNU is actually enhanced in double-stranded DNA versus single-stranded DNA, indicating that steric factors are not significant in this process (*33*). Metha et al. (*36*) showed that MNU alone, or coupled with a specific major groove intercalator agent, might be hydrolyzed in the major groove, and increased the extent of *N*7-guanine methylation as shown by the ratio of *N*7-methylguanine (a major groove lesion) to *N*3-methyladenine (a minor groove lesion). The accessibility of the *N*7 of a central guanine in GGG runs is greater than in other nucleotide triplets; this could explain the pattern observed with S_N1 agents (*37*). However, it is unlikely that only steric effects are responsible for the *N*7-Methylguanine distribution patterns observed with MNU and NDMAOAc. In the same DNA sequence, the 5′-Gs in dG3 or dG4 stretches are accessible to the bulkier DMS, known to react primarily at the *N*7-guanine position in the DNA major groove. The methylation efficiency observed with DMS-induced DNA damage in guanine runs does not support the hypothesis that guanines are more accessible in the middle than in the 5′- or 3′-end.

The high electrostatic potential predicted for guanine runs may account for the sequence selectivity observed with S_N1 and S_N2 agents. The molecular electrostatic potential (MEP) is highest for the *N*7 and O^6 positions of guanines in double- and single-stranded DNA or a single nucleotide (*38*). The effects of the nearest neighbor base pair on the MEP of the *N*7 position of guanine in B-DNA showed that the 5′-guanine in a run of guanines possesses the highest MEP at the *N*7-guanine (*38*). The MEP decreases toward the 3′-guanine. The molecular rationale for the preference of MNU and NDMAOAc for runs of guanines is, therefore, that the positively charged diazonium ion produced is drawn toward the more electronegative guanine *N*7 position on the 5′-end of a guanine run. The distribution patterns of MNU and NDMAOAc-induced DNA damage do not follow this rationale (Figure 5). However, we observed that the distribution pattern obtained with DMS is related to the MEP mentioned above (Figure 5). Fluctuation in the nucleophilicity at the *N*7-guanine sites, as a consequence of subtle sequence-dependent conformational changes that alter base stacking, could account for the methylation pattern. Sugiyama and Saito carried out molecular orbital calculations of stacked DNA bases (*39*). The

ionization potential was estimated for several sets of two stacked nucleobases and several stacked nucleobase pairs. They observed that 70% of the highest occupied molecular orbital is localized on the 5′-guanine of 5′-GG-3′ (*39*). These calculations indicate that the 5′-guanine of 5′-GG-3′ is the most electron-donating site in B-DNA, and suggest that one-electron transfer from DNA to an electron acceptor is more efficient at 5′-GG-3′ sites (*39*).

A rationale for the sequence specificity observed with S_N1 agents was recently proposed by Liang et al. and Dande et al. (*40*, *41*). DNA methylation by MNU was regioselectively inhibited by point substitutions of the zwitterionic pyrimidines. These residues cause a regioselective inhibition of methylation at the *N*7 position of the guanine located 2−3 bp toward the 5′-end of the complementary strand. Moreover, no inhibition was observed for DNA methylation with DMS. Their results suggest that the sequence specificity observed with MNU depends on both the stereoelectronic environment of the guanines and the nature of the methylating agent (*40*, *41*). We propose that these conclusions about the sequence specificity encountered by MNU could also apply to NDMAOAc.

As shown in this study, shielding of DNA by proteins was detected in the c-*jun* promoter of human fibroblasts subjected to methylating agents. c-*jun* is an important component in gene regulation of genes activated during cell response to DNA damage (*42*). As a member of the early-response gene family, c-*jun* is induced within minutes of exposure to alkylating agents (*42*). We observed seven footprints from nucleotides 0 to −199, upstream of the transcription initiation site (Figures 6 and 8 and data not shown). Protein−DNA interactions were detected at the AP-1-like sequence, CCAAT box, the NF-jun sequence, the SP-1 sequence, and a putative RSRF binding site. Similar protein−DNA complexes were observed with MNU and NDMAOAc. These protein−DNA complexes are similar to those observed with DMS, UV, and DNase I (*29*, *43*, *44*). We observed that the presence of transcription factors reduced the level of MNU- or NDMAOAc-induced DNA damage. It would be interesting to determine whether these factors may protect DNA from the other reactive intermediates generated by NNK. Furthermore, a hyperreactive G in cell culture treatment is observed with MNU and NDMAOAc near the RSRF binding site at nucleotide −33 of the transcription initiation site. This hyperreactive site has been reported with DNase I treatment, but not with DMS treatment (*29*, *44*).

The sequence specificity in guanine runs observed with MNU and NDMAOAc (S_N1 agents) is similar in naked DNA and in treated cells. The methylation patterns observed with NDMAOAc or NNK are expected to be identical. Future studies will focus on the second pathway of NNK activation leading to pyridyloxobutylation of the DNA. Taken together, the methylation patterns and the pyridyloxobutylation patterns will help to define the role of each activation pathway of NNK in inducing DNA damage and their relative significance in tobacco-induced lung carcinogenesis. The specificity of NNK may include preferential reaction at GC-rich genomic locations or at guanine runs of genes, resulting ultimately in DNA mutations. Mutations in codon 12 of the K-*ras* gene are present in 24−50% of the human primary adenocarcinomas but are rarely seen in other types of lung tumors (*45*−*47*). These mutations are more common in smokers than in nonsmokers, suggesting that they may be induced by a component of tobacco smoke (*48*). The mutations in the *ras* genes are about 80% G to T transversions and 20% G to A transitions in smokers (*45*). In the *p53* gene, mutations are more frequently G to T transversions (*3*, *45*). Our results show that DNA damage occurs mainly on guanines. The distribution of NDMAOAc-induced guanine methylation also correlates with the mutation spectrum found in lung cancer. In conclusion, NNK-induced DNA damage, generated through the α-methylene hydroxylation leading to methylated bases, could be significant in NNK-induced mutations.

Acknowledgment. This study was supported by Grant CM 063375 from the Medical Research Council of Canada (MRC) to A.C. and by a grant from the Canadian Genetic Diseases Network (MRC/NSERC NCE Program) to R.D. J.-F.C. was recipient of a studentship from Park-Davis Canada, and R.D. is a research scholar of the Cancer Research Society Inc./MRC program. We are grateful to Mrs. Isabelle Paradis and Nancy Dallaire for fibroblast culture and to Mr. Jean-Philippe Therrien for his assistance with the phosphorimager.

References

(1) Holmquist, G. P., and Gao, S. (1997) Somatic mutation theory, DNA repair rates, and the molecular epidemiology of p53 mutations. *Mutat. Res.* **386**, 69−101.

(2) Holmquist, G. P., and Drouin, R. (1998) Cyclobutane dimer frequency and their repair rates drive tumor mutation frequency in p53 genes. In *Landmarks in Photobiology* (Hönigsmann, H., Knobler, R. M., Trautinger, F., and Jori, G., Eds.) pp 396−398, OEMF spa, Milan, Italy.

(3) Greenblatt, M. S., Bennett, W. P., Hollstein, M., and Harris, C. C. (1994) Mutations in the p53 tumor suppressor gene: clues to cancer etiology and molecular pathogenesis. *Cancer Res.* **54**, 4855−4878.

(4) Hecht, S. S., and Hoffmann, D. (1989) The relevance of tobacco-specific nitrosamines to human cancer. *Cancer Surv.* **8**, 273−294.

(5) Fischer, S., Spiegelhalder, B., and Preussmann, R. (1990) Tobacco-specific nitrosamines in European and USA cigarettes. *Arch. Geschwulstforsch.* **60**, 169−270.

(6) Fischer, S., Castonguay, A., Kaisermann, M., Spiegelhalder, B., and Preussmann, R. (1990) Tobacco-specific nitrosamines in Canadian cigarettes. *J. Cancer Res. Clin. Oncol.* **116**, 563−568.

(7) Hecht, S. S. (1998) Biochemistry, biology, and carcinogenicity of tobacco-specific *N*-nitrosamines. *Chem. Res. Toxicol.* **11**, 559−603.

(8) Roller, P. P., Shimp, D. R., and Keefer, L. K. (1975) Synthesis and solvolysis of methyl(acetoxymethyl)nitrosamine. Solution chemistry of the presumed carcinogenic metabolite of dimethylnitrosamine. *Tetrahedron Lett.* **25**, 2065−2068.

(9) Milligan, J. R., Hirani-Hojatti, S., Catz-Biro, L., and Archer, M. C. (1989) Methylation of DNA by three *N*-nitroso compounds: evidence for sequence specific methylation by a common intermediate. *Chem.-Biol. Interact.* **72**, 175−189.

(10) Brisco, W. T., and Cotter, L. E. (1984) The effects of neighboring bases on *N*-methyl-*N*-nitrosourea alkylation of DNA. *Chem.-Biol. Interact.* **52**, 103−110.

(11) Dolan, M. E., Oplinger, M., and Pegg, A. E. (1988) Sequence specificity of guanine alkylation and repair. *Carcinogenensis* **9**, 2139−2143.

(12) Wurdeman, R. L., and Gold, B. (1988) The effect of DNA sequence, ionic strength, and cationic DNA affinity binders on the methylation of DNA by *N*-methyl-*N*-nitrosourea. *Chem. Res. Toxicol.* **1**, 146−147.

(13) Wurdeman, R. L., Church, R. L., and Gold, B. (1989) DNA methylation by *N*-methyl-*N*-nitrosourea, *N*-methyl-*N*′-nitro-*N*-nitrosoguanidine, *N*-nitroso(acetoxyethyl)methylamine, and diazomethane: mechanism for the formation of *N*7-methylguanine in sequence-characterized 5′-^{32}P-end labeled DNA. *J. Am. Chem. Soc.* **111**, 6408−6412.

(14) Said, B., and Shank, R. C. (1991) Nearest neighbor effects on carcinogen binding to guanine runs in DNA. *Nucleic Acids Res.* **19**, 1311−1316.

(15) Shoukry, S., Anderson, M. W., and Glickman, B. W. (1993) Use of fluorescently tagged DNA and an automated DNA sequencer

for the comparison of the sequence selectivity of SN1 and SN2 alkylating agents. *Carcinogenesis* **14**, 155−157.
(16) Brisco, W. T., and Cotter, L. E. (1985) DNA sequence has an effect on the extent and kinds of alkylation of DNA by a potent carcinogen. *Chem.-Biol. Interact.* **56**, 321−331.
(17) Warpehoski, M. A., and Hurley, L. H. (1988) Sequence specificity of DNA covalent modification. *Chem. Res. Toxicol.* **1**, 315−333.
(18) Pfeifer, G. P., Drouin, R., and Holmquist, G. P. (1993) Detection of DNA adducts at the DNA sequence level by ligation-mediated PCR. *Mutat. Res.* **288**, 39−46.
(19) Drouin, R., Rodriguez, H., Holmquist, G. P., and Akman, S. A. (1996) Ligation-mediated PCR for analysis of oxidative DNA damage. In *Technologies for Detection of DNA Damage and Mutations* (Pfeifer, G. P., Ed.) pp 211−225, Plenum Press, New York.
(20) Pfeifer, G. P., and Riggs, A. D. (1993) Genomic footprinting by ligation mediated polymerase chain reaction. PCR protocols: current methods and applications. *Methods Mol. Biol.* **15**, 153−168.
(21) Pfeifer, G. P., and Riggs, A. D. (1993) Genomic sequencing. DNA sequencing protocols. *Methods Mol. Biol.* **23**, 169−181.
(22) Peterson, L. A., Liu, X.-K., and Hecht, S. S. (1993) Pyridyloxobutyl DNA adducts inhibit the repair of O^6-methylguanine. *Cancer Res.* **53**, 2780−2785.
(23) Drouin, R., Gao, S., and Holmquist, G. P. (1996) Agarose gel electrophoresis for DNA damage analysis. In *Technologies for Detection of DNA Damage and Mutations* (Pfeifer, G. P., Ed.) pp 37−43, Plenum Press, New York.
(24) Maxam, A. M., and Gilbert, W. (1980) Sequencing end-labeled DNA with base-specific chemical cleavage. *Methods Enzymol.* **65**, 499−560.
(25) Iverson, B. L., and Dervan, P. B. (1987) Adenine specific DNA chemical sequencing reaction. *Nucleic Acids Res.* **19**, 7823−7830.
(26) Tornaletti, S., and Pfeifer, G. P. (1996) Ligation-mediated PCR for analysis of UV damage. In *Technologies for Detection of DNA Damage and Mutations* (Pfeifer, G. P., Ed.) pp 199−209, Plenum Press, New York.
(27) Törmänen, V. T., and Pfeifer, G. P. (1992) Mapping of UV photoproducts within ras proto-oncogenes in UV-irradiated cells: correlation with mutations in human skin cancer. *Oncogene* **7**, 1729−1736.
(28) Tornaletti, S., Rozek, D., and Pfeifer, G. P. (1993) The distribution of UV photoproducts along the human p53 gene and its relation to mutations in skin cancer. *Oncogene* **8**, 2051−2057 (published erratum appears on page 3469 of the December 1993 issue of *Oncogene*).
(29) Rozek, D., and Pfeifer, G. P. (1993) In vivo protein-DNA interactions at the *c-jun* promoter: preformed complexes mediate the UV response. *Mol. Cell. Biol.* **13**, 5490−5499.
(30) Mattes, W. B., Hartley, J. A., and Kohn, K. W. (1986) Mechanism of DNA strand breakage by piperidine at sites of *N*7-alkylguanines. *Biochim. Biophys. Acta* **868**, 71−76.
(31) Pfeifer, G. P., Tanguay, R. L., Steigerwald, S. D., and Riggs, A. D. (1990) In vivo footprint and methylation analysis by PCR-aided genomic sequencing: comparison of active and inactive X chromosomal DNA at the CpG island and promoter of human PGK-1. *Genes Dev.* **4**, 1277−1287.
(32) Beranek, D. T. (1990) Distribution of methyl ethyl adducts following alkylation with monofunctional alkylating agents. *Mutat. Res.* **231**, 11−30.
(33) Wurdeman, R. L., Douskey, M. C., and Gold, B. (1993) DNA methylation by *N*-methyl-*N*-nitrosourea: methylation pattern changes in single- and double-stranded DNA, and in DNA with mismatched or bulged guanines. *Nucleic Acids Res.* **21**, 4975−4980.
(34) Hartley, J. A., Gibson, N. W., Kohn, K. W., and Mattes, W. B. (1986) DNA sequence selectivity of guanine-N7 alkylation by three antitumor chlorethylating agents. *Cancer Res.* **46**, 1943−1947.
(35) Hartley, J. A. (1990) Mechanisms of DNA sequence selective modifications by alkylating agents. In *Molecular Basis of Specificity in Nucleic Acid-Drug Interaction* (Pullman, B., and Jortner, J., Eds.) pp 513−530, Kluwer Academic Publishers, Dordrecht, The Netherlands.
(36) Mehta, P., Church, K., Williams, J., Chen, F. X., Encell, L., Shuker, D. E., and Gold, B. (1996) The design of agents to control DNA methylation adducts. Enhanced major groove methylation of DNA by an *N*-methyl-*N*-nitrosourea functionalized phenyl neutral red intercalator. *Chem. Res. Toxicol.* **9**, 939−948.
(37) Lavery, R., Pullman, A., and Pullman, B. (1981) Steric accessibility of reactive centers in B-DNA. *Int. J. Quantum Chem.* **20**, 49−62.
(38) Pullman, A., and Pullman, B. (1981) Molecular electrostatic potential of the nucleic acids. *Q. Rev. Biophys.* **14**, 289−380.
(39) Sugiyama, H., and Saito, I. (1996) Theoretical studies of GG-specific photocleavage of DNA via electron transfer: significant lowering of ionization potential and 5′-localization of HOMO of stacked GG bases in B-form DNA. *J. Am. Chem. Soc.* **118**, 7063−7068.
(40) Liang, G., Encell, L., Nelson, M. G., Switzer, C., and Gold, B. (1995) Role of electrostatics in the sequence-selective reaction of charged alkylating agents with DNA. *J. Am. Chem. Soc.* **117**, 10135−10136.
(41) Dande, P., Liang, G., Chen, F. X., Roberts, C., Nelson, M. G., Hashimoto, H., Switzer, C., and Gold, B. (1997) Regioselective effect of zwitterionic DNA substitutions on DNA alkylation: evidence for a strong side chain orientational preference. *Biochemistry* **36**, 6024−6032.
(42) Friedberg, E. C., Walker, G. C., and Siede, W. (1995) Regulatory responses to DNA-damaging agents in eukaryotic cells. In *DNA Repair and Mutagenesis* (Friedberg, E. C., Walker, G. C., and Siede, W., Eds.) pp 595−632, American Society for Microbiology, Washington, DC.
(43) Tornaletti, S., and Pfeifer, G. P. (1995) UV light as a footprinting agent: modulation of UV-induced DNA damage by transcription factors bound at the promoters of three human genes. *J. Mol. Biol.* **249**, 714−728.
(44) Rozek, D., and Pfeifer, G. P. (1995) In vivo protein-DNA interactions at the c-jun promoter in quiescent and serum-stimulated fibroblasts. *J. Cell Biochem.* **57**, 479−487.
(45) Rodenhuis, S., and Slebos, R. J. (1992) Clinical significance of ras oncogene activation in human lung cancer. *Cancer Res.* **52**, 2665s−2669s.
(46) Mills, X. E., Fishman, C. L., Rom, W. N., Dubin, N., and Jacobson, D. R. (1995) Increased prevalence of K-ras oncogene mutations in lung adenocarcinoma. *Cancer Res.* **55**, 1444−1447.
(47) Westra, W. H., Baas, I. O., Hruban, R. H., Askin, F. B., Wilson, K., Offerhaus, G. J. A., and Slebos, R. J. C. (1996) K-ras oncogene activation in atypical alveolar hyperplasias of the human lung. *Cancer Res.* **56**, 2224−2228.
(48) Westra, W. H., Slebos, R. J. C., Offerhaus, C. J. A., Goodman, S. N., Evers, S. G., Kensler, T. W., Askin, F. B., Rodenhuis, S., and Hruban, R. H. (1993) K-ras oncogene activation in lung adenocarcinomas from former smokers. *Cancer* **72**, 432−438.

TX990025F